Silicon Defects

DOI: 10.1002/anie.201100733

Activation Energies for Diffusion of Defects in Silicon: The Role of the Exchange-Correlation Functional**

Stefan K. Estreicher, Daniel J. Backlund, Christian Carbogno, and Matthias Scheffler*

Dedicated to the Fritz Haber Institute, Berlin, on the occasion of its 100th anniversary

The electrical, optical, and magnetic properties of semiconductors are controlled by the defects and impurities they contain.[1–4] Device manufacturing requires placing specific impurities at specific sites in the crystal while avoiding their diffusion and preventing unwanted contamination. But device processing includes annealing steps, and defects can diffuse within the annealing time. Many defects have a donor and/or acceptor level in the forbidden energy gap, and their diffusivity depends on their charge state, in other words, on the Fermi level or the exposure to photons at or above the bandgap energy. A defect-related gap level may also shift from the gap into a band (or vice versa) during a diffusion step, which can lead to a change in the charge state of the defect.

Herein we focus on the simple issue of defect diffusion by thermally stimulated "over-the-barrier" hopping. We compare the activation energies (E_a) obtained with the same supercell, pseudopotentials, basis set, and k-point sampling, but different exchange-correlation functionals (E_{xc}). The charge and spin are fixed in each calculation.

In harmonic transition-state theory, the diffusivity of a defect is given by $D(T) = D_0 \exp\{-E_a/k_B T\}$ [$cm^2 s^{-1}$], where the prefactor D_0 contains the attempt frequency,[5] E_a is the total energy difference between the saddle point and the minimum of the potential-energy surface, and k_B is the Boltzmann constant.

Experimentally determined Arrhenius plots ($\log D$ vs. $1/T$) are often very close to a straight line. A fit produces E_a (negative of the slope) and D_0 (y-intercept for $T^{-1} \rightarrow 0$). For defects in semiconductors, the almost perfectly constant slope of Arrhenius plots over wide ranges of temperatures[6–8] justifies the assumption that the temperature dependence of the vibrational frequencies, which enter in the prefactor D_0, can be safely ignored.

[*] Prof. Dr. S. K. Estreicher
Physics Department, Texas Tech University
Lubbock, TX 79409-1051 (USA)
E-mail: stefan.estreicher@ttu.edu
Dr. D. J. Backlund
Texas Tech University Health Sciences Center
IT–Room 1C384, Lubbock, TX 79409 (USA)
Dr. C. Carbogno, Prof. Dr. M. Scheffler
Fritz-Haber-Institut der Max-Planck Gesellschaft
Faradayweg 4–6, 14195 Berlin-Dahlem (Germany)

[**] The work of S.K.E. is supported in part by grant D-1126 from the R. A. Welch Foundation and by the Silicon Solar Consortium.

Ab initio molecular dynamics (MD) simulations of $D(T)$ require very long simulation times.[9] Direct calculations of activation energies are much faster, but they require the knowledge of the diffusion path and saddle point. In any case, the errors associated with local and semilocal exchange-correlation functionals in density functional theory (DFT) are different at minima and saddle-point configurations as the Kohn–Sham orbitals are differently extended,[10] sometimes leading to underestimations of E_a.

In order to quantify these arguments, we performed nudged elastic band (NEB)[11–13] calculations with various E_{xc} functionals. In the Kohn–Sham formulation of DFT, the (electronic) many-body problem is mapped exactly onto a single-particle Hamiltonian. All many-body effects are subsumed into an exchange-correlation potential. Were this functional known exactly, the solution of the single-particle equations would yield the exact ground-state electron density n of the many-body system. But the exact $E_{xc}[n]$ (and $V_{xc}[n] = \delta E_{xc}/\delta n$) is not known. Useful approximations to it have been proposed over the years.

The local density approximation (LDA)[14] is derived from the E_{xc} of a homogeneous electron gas. It reproduces satisfactorily the basic geometric properties of bulk structures with a few percent error margins.[15] However, it is not uncommon to find errors of the order of 20% for the cohesive energies of solids while the adsorption energies of molecules at surfaces can only be determined with limited accuracy.[16,17]

Functionals based on the generalized gradient approximation (GGA) partially correct for these flaws[15–17] since they account for changes in the electronic density in a semilocal fashion. The most prominent one, the Perdew–Burke–Ernzerhof (PBE) functional,[18] is derived from first principles. All the parameters are basically fundamental constants, but some flexibility remains in the formulation of the exchange part. The "simplest conceivable dimensionally consistent expression" was selected for the exchange enhancement factor, previously derived by Becke.[19] The parameter κ was chosen such that the exchange interaction complies with the local Lieb–Oxford inequality, which ensures that the integrated Lieb–Oxford condition[20] is fulfilled.

Zhang and Yang[21] pointed out that the local Lieb–Oxford inequality is a sufficient but not a necessary condition for the fulfillment of the integrated Lieb–Oxford condition. They proposed a revised PBE functional (revPBE), which is not based on the local Lieb–Oxford inequality. The parameter κ is such that the total energies computed by optimized exchange potential simulations[22] for isolated atoms are reproduced.

The revPBE functional still fulfills the integrated Lieb–Oxford condition, albeit not by construction.

The RPBE functional[17] uses a slightly different functional form for the exchange enhancement factor but is in all other respects identical to the revPBE functional. Both revPBE and RPBE typically yield significantly better atomization and adsorption energies for molecules than PBE does,[16,17] in particular in systems that include oxygen (a review of electronic structures methods is given in Ref. [23]).

We study here the impact of E_{xc} on the activation energies of two types of defects in Si. Atomic-like impurities exhibit little covalent overlap with the host crystal and induce very small distortions: tetrahedral interstitial hydrogen (H_T^0 or H_T^-), interstitial iron (Fe_i^+ or Fe_i^0), or nickel (Ni_i^0). Strongly bound impurities interact covalently with the host crystal, which often undergoes substantial distortions: bond-centered hydrogen (H_{BC}^+ or H_{BC}^0), interstitial oxygen (O_i^0), or Si itself (self-diffusion).

The diffusion paths and saddle points are obtained with the NEB method for each charge state of each defect and for each E_{xc}. When several paths are a priori possible, the NEB calculations are repeated with intermediate configurations in different crystallographic planes. In all examples considered here, these calculations converged toward the same minimum-energy path.

Our electronic structure and ab initio molecular dynamics simulations[24] employ the SIESTA code.[25,26] The host crystal is represented by a 64 host-atom periodic supercell. This relatively small cell size was chosen because the NEB[11–13] calculations require substantial computer time. The lattice constant a_L of the perfect cell is optimized in each charge state and for each E_{xc}. For example, in the neutral charge state, the lattice constants are 5.383647 Å (LDA), 5.465318 Å (PBE), 5.491275 Å (revPBE), and 5.499234 Å (RPBE). Note that supercells with a poorly optimized lattice constant have residual strain which causes poor convergence of NEB calculations. The defect geometries are optimized with a conjugate gradient algorithm until the maximum force component is smaller than 0.005 eV Å^{-1}. A $2\times2\times2$ Monkhorst–Pack[27] mesh is used to sample the Brillouin zone. The electronic core regions are described with (optimized[28]) ab initio pseudopotentials,[29,30] recompiled for each V_{xc}.

The valence regions are treated with first-principles (spin) DFT within LDA,[31,32] PBE,[18] revPBE,[22] and RPBE.[17] The basis sets for the valence states are linear combinations of numerical atomic orbitals:[33,34] double-zeta sets for elements in the first and second row of the periodic table, plus polarizations functions for Si. The basis sets for Fe has two sets of valence s and d functions, and one set of p functions. These basis sets have been shown to be reliable when calculating many properties of defects.[35–38] The charge density is projected on a real-space grid with an equivalent cutoff of 350 Ryd to calculate the exchange-correlation and Hartree potentials.

Our implementation of the NEB method uses the climbing image method[12] for finding the saddle points. Local tangents are estimated using the improved-tangent formalism.[13] The springs connecting the images have a spring constant of 0.1 eV Å^{-1}. The number of images is determined in part by the length of the diffusion path, in part by the number of initial intermediate configurations needed, and in part by experience. Some of the calculations require only 7 images, but 15 are used for Si self-diffusion. The converged diffusion path is the one for which the maximum force component perpendicular to the path at each image is less than 0.04 eV Å^{-1}.

As impurities, atomic-like interstitials exhibit little covalent overlap with the host crystal, as shown by very small overlap populations[39] between H_T^0, H_T^-, Fe_i^+, Fe_i^0, or Ni_i^0 and the host crystal. Only small relaxations (of the order of 0.1 Å) of the Si nearest neighbors (NNs) occur. All the impurities in this section are stable at the tetrahedral interstitial (T) site and diffuse along a straight line from one T site to the next with the saddle point at the hexagonal interstitial site.

The stable states of hydrogen in Si are H_{BC}^+ (in p-Si) and H_T^- (in n-Si).[50] The neutral impurities H_T^0 and H_{BC}^0 are metastable.[51] The activation energy for diffusion of H_T^0 is not known experimentally. The present calculations produce the very small value of 0.18 eV. However, H has three vibrational modes at the T site (of the order of 800 cm^{-1}) but only two at the saddle point. If one includes the difference in the zero-point energies between the minimum and saddle-point configurations ($\approx$0.1 eV), the actual barrier drops to about 0.08 eV.[52] Two experimental studies[40,41] in the range 65 K to room temperature support such a small value.

The fit of the diffusivity of D_T^- in P-doped Si in the narrow range 300 to 320 K produced $E_a = 0.7$ eV,[43] substantially higher than the value we calculate (Table 1). This could be due to an unexpected problem with the calculation. It is also possible that these experiments involve trap-limited (rather than free) diffusion, as D_T^- hops from P^+ to P^+ impurities in the Schottky diodes. The 0.7 eV would then be the dissociation energy of the $\{D^-P^+\}$ pair rather than the activation energy for diffusion of D_T^- in impurity-free Si.

Table 1: Calculated and experimental activation energies E_a [eV] for atomic-like interstitial impurities in Si.

Impurity	LDA	PBE	revPBE	RPBE	Experiment
H_T^0	0.16	0.17	0.18	0.18	see text[40–42]
H_T^-	0.37	0.41	0.43	0.43	0.7[43]
Fe_i^+	0.82	0.71	0.74	0.69	0.69[44–47]
Fe_i^0	0.88	0.85	0.83	0.86	0.84[44–47]
Ni_i^0	0.27	0.23	0.21	0.21	see text[48,49]

Fe is a very common impurity in Si and its properties have been the subject of extensive reviews.[44] It has a deep donor level in the gap, and is therefore Fe_i^+ in p-Si and Fe_i^0 in n-Si, with spin $^3/_2$ and 1, respectively. The E_a is charge-state dependent[45–47] and the accepted values[44] match best the ones at the RPBE level, but PBE and revPBE predict similar values.

The donor (acceptor) level of Ni_i is predicted[48] to be just below the top (above the bottom) of the valence (conduction) band, at both the LDA and GGA levels. Thus, Ni_i is predicted to be in the zero charge state for all positions of the Fermi

level. Its E_a is tricky to measure, and the published experimental values vary from 0.13 to 4.24 eV![49] Our RPBE prediction, 0.21 eV, is only slightly higher than for that for Cu_i^+, 0.18 eV,[48] which matches the experimental value.[53]

The E_a values of atomic-like impurities are rather well described even at the LDA level. The worst LDA values occur for Fe_i, which is only approximately "atomic-like" since it exhibits more covalent overlap with the host crystal than the other impurities considered in this section. The difference between the LDA and RPBE results is typically less than 0.1 eV.

Strongly bound impurities overlap considerably with the host crystal, which itself is often distorted even at the minimum of the potential surface. For example, bond-centered-type interstitials involve Si NN displacements of 0.5 to 0.7 Å while substitutional impurities exhibit strong covalent overlap with their Si NNs. The distortions are more severe at the saddle point, which also involves unusual coordination numbers. The NEB calculations require the use at least one intermediate configuration. For all the defects considered here, the NEB calculations with different initial intermediate configurations converge toward the same path.

The diffusion of H_{BC}^+ in Si has been studied since 1956,[54] although the nature of the diffusing species was not recognized at that time. These data produced $E_a = 0.48$ eV. They were taken not far from the melting point of Si. At lower temperatures,[55] the trapping of H at impurities complicates the measurements, but EPR data at 80 K have confirmed that a single jump also occurs with the activation energy of 0.48 eV.[56] The activation energy of the metastable H_{BC}^0 is not known experimentally. We find it to be lower than that of H_{BC}^+, as the extra electron helps stabilize the saddle-point configuration.

The case of O_i^0 is of special interest because of the considerable strength of the Si–O bond. The parameterization of the RPBE functional itself was designed in part to better describe the adsorption of O on various surfaces.[17] O_i is at a slightly puckered bond-centered site, strongly bound to two Si neighbors. The experimental E_a is close to 2.5 eV.[57,59] Numerous authors have predicted a wide range of E_a values[59] obtained at various levels of theory. A careful attempt to identify the saddle point from first principles at the LDA level[61] yielded the activation energy of 1.6 eV, close to the LDA value in Table 2. These calculations[61] were done in a 32 Si-atom supercell with a single k point and geometries optimized to a maximum force component of 0.5 eV Å^{-1}.

The substantial discrepancy between the LDA result and the experimental activation energy is largely—but not fully—corrected with the RPBE functional. The initial, saddle-point, and final configurations for the diffusion of O_i^0 are shown in Figure 1 and the potential energy surface in Figure 2.

In the case of Si^0 self-diffusion, two adjacent Si atoms exchange position. NEB calculations with initial intermediate configurations with ⟨110⟩ or ⟨100⟩ symmetry converged toward the same path and saddle point, where the two Si atoms are oriented along a ⟨110⟩ direction (Figure 3).

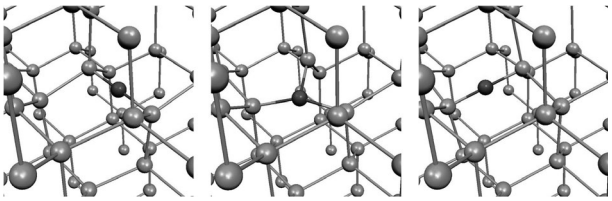

Figure 1. Initial (left), saddle-point (middle), and final (right) configurations for the diffusion of O_i^0.

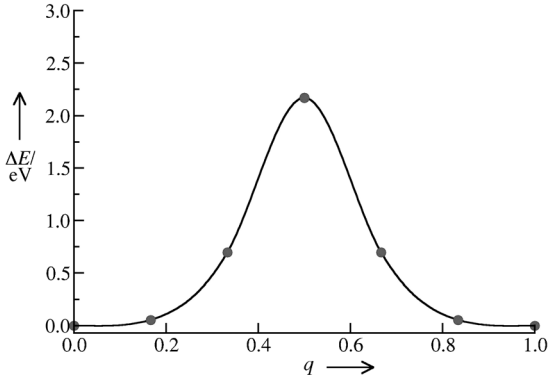

Figure 2. Potential-energy surface for the diffusion of O_i^0 obtained with the RPBE functional along a generalized coordinate q. The dots show the images used in the NEB calculations.

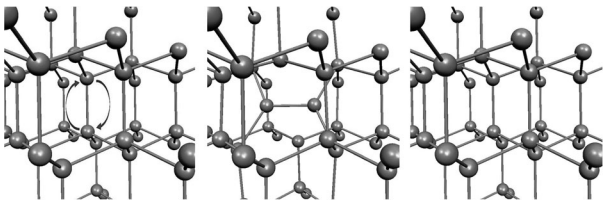

Figure 3. Initial or final (left or right), and saddle-point (middle) configurations for self-diffusion of Si^0. At the saddle point, the two Si atoms switching position are oriented along a <110> direction.

Table 2: Calculated and experimental activation energies [eV] for strongly bound impurities in Si.

Impurity	LDA	PBE	revPBE	RPBE	Experiment
H_{BC}^+	0.22	0.39	0.45	0.47	0.48[54–56]
H_{BC}^0	0.19	0.31	0.35	0.38	–
O_i^0	1.79	2.01	2.12	2.18	2.44–2.56[57–59]
Si^0 self-diffusion	4.31	4.49	4.56	4.58	4.56[60]

The self-diffusion experiments[60] involved Si layers of highly enriched ^{28}Si separated by layers of natural abundance Si (^{nat}Si). The diffusion of various impurities present in the sample, including Si isotopes, was monitored by secondary-ion mass spectrometry following anneals at various temperatures. The experimental E_a for self-diffusion, 4.56 eV, is closely reproduced by both the revPBE and RPBE calculations (Figure 4).

The prediction of the activation energy for diffusion of a defect in covalent materials such as Si requires knowing the

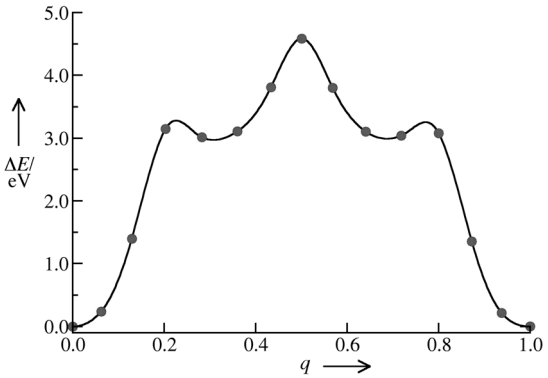

Figure 4. Potential-energy surface for the self-diffusion in Si obtained with the RPBE functional along a generalized coordinate q. The dots show the images used in the NEB calculations.

migration path and calculating the total energies at the minimum as well as saddle-point configurations with the same level of accuracy. In the examples considered, the paths calculated with various E_{xc} values are almost indistinguishable from each other. However, the theoretical errors in the total energies are different at the minimum and saddle point, leading to variations in E_a with E_{xc}.

The results show that the GGA functionals are superior to the LDA one for the description of the diffusion process. RPBE systematically provides the most (and LDA the least) accurate activation energies. However, all the GGA functionals give comparable results, as expected since the differences between PBE, revPBE, and RPBE are subtle.

The errors depend on how much the covalent bonds at the saddle point are strained, on the bond strengths, and on how far the saddle-point configuration is from a chemical equilibrium. The examples selected here illustrate that the activation energies of atomic-like interstitials vary little (≈ 0.06 eV) with E_{xc}, but those of strongly bound impurities are much more sensitive to it (0.3–0.5 eV). The accuracy problem arises when strong bonds are cut and new ones formed. Then neither LDA nor GGA functionals are guaranteed to give a reliable description.

Note that many diffusion experiments are performed at high temperatures while our NEB calculations are done at 0 K. However, the thermal expansion coefficient of Si is very small. For example, a_L increases from 5.430 to 5.445 Å in the range 0 to 740 °C.[62] This small change does not affect the calculated activation energies and is consistent with the almost perfectly constant slope of Arrhenius plots over wide ranges of temperatures.

Received: January 28, 2011
Published online: May 20, 2011

Keywords: defect diffusion · density functional calculations · exchange-correlation functional · semiconductors · silicon

[1] H. J. Queisser, E. E. Haller, *Science* **1998**, *281*, 945 – 950.
[2] H. R. Huff, *Encyclopedia of Applied Physics*, *Vol. 17*, VCH Publ., NewYork, **1996**, pp. 437 – 475.
[3] H. Temkin, S. K. Estreicher in *Encyclopedia of Chemical Physics and Physical Chemistry*, *Vol. III* (Ed.: J. H. Moore, N. D. Spencer), IOP, Bristol, **2002**, pp. 2567 – 2588.
[4] E. E. Haller, *Science* **2006**, *311*, 547 – 553.
[5] C. Ratsch, M. Scheffler, *Phys. Rev. B* **1998**, *58*, 13163 – 13167.
[6] Y. Fukai, H. Sugimoto, *Adv. Phys.* **1985**, *34*, 263 – 324.
[7] S. J. Pearton, J. W. Corbett, M. Stavola, *Hydrogen in Crystalline Semiconductors*, Springer, Berlin, **1992**, chap. 9.
[8] E. R. Weber, *Appl. Phys. A* **1983**, *30*, 1 – 22.
[9] F. Buda, G. L. Chiarotti, R. Car, *Phys. Rev. Lett.* **1989**, *63*, 294 – 297.
[10] A. J. Cohen, P. Mori-Sánchez, W. Yang, *Science* **2008**, *321*, 792 – 794.
[11] G. Mills, H. Jonsson, *Phys. Rev. Lett.* **1994**, *72*, 1124 – 1127.
[12] G. Henkelman, B. P. Uberuaga, H. Jonsson, *J. Chem. Phys.* **2000**, *113*, 9901 – 9904.
[13] G. Henkelman, H. Jonsson, *J. Chem. Phys.* **2000**, *113*, 9978 – 9985.
[14] W. Kohn, *Rev. Mod. Phys.* **1999**, *71*, 1253 – 1266.
[15] V. Staroverov, G. Scuseria, J. Tao, J. Perdew, *Phys. Rev. B* **2004**, *69*, 075102.
[16] S. Kurth, J. P. Perdew, P. Blaha, *Int. J. Quantum Chem.* **1999**, *75*, 889 – 894.
[17] B. Hammer, L. Hansen, J. K. Nørskov, *Phys. Rev. B* **1999**, *59*, 7413 – 7421.
[18] J. P. Perdew, K. Burke, M. Ernzerhof, *Phys. Rev. Lett.* **1996**, *77*, 3865 – 3868.
[19] A. Becke, *J. Chem. Phys.* **1986**, *84*, 4524 – 4529.
[20] E. Lieb, S. Oxford, *Int. J. Quantum Chem.* **1981**, *19*, 427 – 439.
[21] Y. Zhang, W. Yang, *Phys. Rev. Lett.* **1998**, *80*, 890 – 893.
[22] E. Engel, S. H. Vosko, *Phys. Rev. A* **1993**, *47*, 2800 – 2811.
[23] A. Tkatchenko, L. Romaner, O. T. Hofmann, E. Zojer, C. Ambrosch-Draxl, M. Scheffler, *Bull. Mater. Res. Soc.* **2010**, *35*, 435 – 442.
[24] *Theory of Defects in Semiconductors* (Ed.: D. A. Drabold, S. K. Estreicher), Springer, Berlin, **2007**.
[25] D. Sánchez-Portal, P. Ordejón, E. Artacho, J. M. Soler, *Int. J. Quantum Chem.* **1997**, *65*, 453 – 461.
[26] E. Artacho, D. Sánchez-Portal, P. Ordejón, A. García, J. M. Soler, *Phys. Status Solidi B* **1999**, *215*, 809 – 817.
[27] H. J. Monkhorst, J. D. Pack, *Phys. Rev. B* **1976**, *13*, 5188 – 5192.
[28] V. L. Moruzzi, C. B. Sommers, *Calculated Electronic Properties of Ordered Alloys: a Handbook*, World Scientific, Singapore, **1995**.
[29] N. Troullier, J. L. Martins, *Phys. Rev. B* **1991**, *43*, 1993 – 2006.
[30] L. Kleinman, D. M. Bylander, *Phys. Rev. Lett.* **1982**, *48*, 1425 – 1428.
[31] D. M. Ceperley, B. J. Adler, *Phys. Rev. Lett.* **1980**, *45*, 566 – 569.
[32] S. Perdew, A. Zunger, *Phys. Rev. B* **1981**, *23*, 5048 – 5079.
[33] O. F. Sankey, D. J. Niklevski, *Phys. Rev. B* **1989**, *40*, 3979 – 3995.
[34] O. F. Sankey, D. J. Niklevski, D. A. Drabold, J. D. Dow, *Phys. Rev. B* **1990**, *41*, 12750 – 12759.
[35] D. West, S. K. Estreicher, *Phys. Rev. Lett.* **2006**, *96*, 115504.
[36] S. K. Estreicher, M. Sanati, D. West, F. Ruymgaart, *Phys. Rev. B* **2004**, *70*, 125209.
[37] M. Sanati, S. K. Estreicher, M. Cardona, *Solid State Commun.* **2004**, *131*, 229 – 233.
[38] D. J. Backlund, S. K. Estreicher, *Phys. Rev. B* **2010**, *81*, 235213.
[39] W. J. Hehre, L. Radom, P. v. R. Schleyer, J. A. Pople, *Ab-initio molecular orbital theory*, Wiley, New York, **1986**.
[40] C. Langpape, S. Fabian, C. Klatt, S. Kalbitzer, *Appl. Phys. A* **1997**, *64*, 207 – 210.
[41] K. Bonde Nielsen, B. Bech Nielsen, J. Hansen, E. Andersen, J. U. Andersen, *Phys. Rev. B* **1999**, *60*, 1716 – 1728.
[42] K. Bonde Nielsen, L. Dobaczewski, S. Søgård, B. Bech Nielsen, *Phys. Rev. B* **2002**, *65*, 075205.
[43] N. M. Johnson, C. Herring, *Phys. Rev. B* **1992**, *46*, 15554 – 15557.

[44] A. A. Istratov, H. Hieslmair, E. R. Weber, *Appl. Phys. A* **1999**, *69*, 13 – 44.
[45] T. Heiser, A. Mesli, *Appl. Phys. Lett.* **1991**, *58*, 2240 – 2242.
[46] T. Heiser, A. Mesli, *Phys. Rev. Lett.* **1992**, *68*, 978 – 981.
[47] H. Takahashi, M. Suezawa, K. Sumino, *Phys. Rev. B* **1992**, *46*, 1882 – 1885.
[48] D. J. Backlund, S. K. Estreicher, *Phys. Rev. B* **2010**, *81*, 235213.
[49] F. H. M. Spit, D. Gupta, K. N. Tu, *Phys. Rev. B* **1988**, *39*, 1255 – 1260.
[50] C. G. Van de Walle, Y. Bar-Yam, S. T. Pantelides, *Phys. Rev. Lett.* **1988**, *60*, 2761 – 2764.
[51] T. L. Estle, S. K. Estreicher, D. S. Marynick, *Hyperfine Interact.* **1986**, *32*, 637 – 639; T. L. Estle, S. K. Estreicher, D. S. Marynick, *Phys. Rev. Lett.* **1987**, *58*, 1547 – 1550.
[52] S. K. Estreicher, M. Sanati, *Physica B* **2006**, *374 – 375*, 363 – 367.
[53] A. A. Istratov, C. Flink, H. Hieslmair, E. R. Weber, T. Heiser, *Phys. Rev. Lett.* **1998**, *81*, 1243 – 1246.
[54] A. Van Wieringen, N. Warmoltz, *Physica* **1956**, *22*, 849 – 865.
[55] C. H. Seager, R. A. Anderson, *Appl. Phys. Lett.* **1988**, *53*, 1181 – 1184.
[56] Y. V. Gorelkinskii, N. N. Nevinnyi, *Physica B* **1991**, *170*, 155 – 167.
[57] J. W. Corbett, R. S. McDonald, G. W. Watkins, *J. Phys. Chem. Solids* **1964**, *25*, 873 – 879.
[58] U. Gösele, T. Y. Tan, *Appl. Phys. A* **1982**, *28*, 79 – 92.
[59] *Oxygen in Silicon* (Ed.: F. Shimura), Academic, San Diego, **1994**.
[60] H. Bracht, H. H. Silvestri, I. D. Sharp, E. E. Haller, *Phys. Rev. B* **2007**, *75*, 035211.
[61] M. Ramamoorthy, S. T. Pantelides, *Phys. Rev. Lett.* **1996**, *76*, 267 – 270.
[62] *Data in Science and Technology: Semiconductors*, (Ed.: O. Madelung), Springer, Berlin, **1991**, p. 16.

